

SELF-CONSISTENT GRAVITATIONAL CHAOS

David Merritt and Monica Valluri

Rutgers University, New Brunswick, NJ

Abstract: The motion of stars in the gravitational potential of a triaxial galaxy is generically chaotic. However, the timescale over which the chaos manifests itself in the orbital motion is a strong function of the degree of central concentration of the galaxy. Here, chaotic diffusion rates are presented for orbits in triaxial models with a range of central density slopes and nuclear black-hole masses. Typical diffusion times are found to be less than a galaxy lifetime in triaxial models where the density increases more rapidly than $\sim r^{-1}$ at the center, or which contain black holes with masses that exceed $\sim 0.1\%$ of the galaxy mass. When the mass of a central black hole exceeds roughly $0.02 M_{gal}$, there is a transition to global stochasticity and the galaxy evolves to an axisymmetric shape in little more than a crossing time. This rapid evolution may provide a negative feedback mechanism that limits the mass of nuclear black holes to a few percent of the stellar mass of a galaxy.

1. Introduction

The gravitational force that determines the motion of a star in a galaxy has two components: the smooth force generated by the overall mass distribution, and the non-smooth force that results from close encounters between individual stars. The relative importance of the two components after one orbital period is roughly equal to $0.1N/\log N$, where N is the number of stars in the galaxy.¹ For a typical galaxy with $N \approx 10^{11}$ stars, close encounters between stars are unimportant and the dynamics are essentially collisionless, at least over timescales of $10^2 - 10^3$ orbital periods that correspond to galaxy lifetimes.

Motion in a smooth gravitational field becomes quite simple if the number of isolating integrals equals or exceeds the number of degrees of freedom, and much work in galactic dynamics has focussed on finding integrable or near-integrable models for galactic potentials.² Kuzmin^{3,4} showed that there is a unique, ellipsoidally-stratified mass model for which the corresponding potential has three global integrals of the motion, quadratic in the velocities. Kuzmin's model – explored in detail by de Zeeuw,⁵ who christened it the “Perfect Ellipsoid” – has a large, constant-density core in which the orbital motion is that of a 3-D harmonic oscillator. Every orbit in the core of the Perfect Ellipsoid fills a rectangular parallelepiped, or “box.” At higher energies in the Perfect Ellipsoid, box orbits persist, and three new orbit families appear: the “tubes,” orbits that

preserve the direction of their motion around either the long or short axis of the figure. Tube orbits respect an integral of the motion analogous to the angular momentum, and hence – unlike box orbits – avoid the center. When two of the axis lengths of an ellipsoidal model are equal, the box orbits disappear, and all trajectories belong to a single family of tube orbits that circulate about the axis of symmetry. Thus, box orbits are uniquely associated with the triaxial geometry.

Unfortunately, the Perfect Ellipsoid does not look very much like real elliptical galaxies. Its density falls off as $\rho \propto r^{-4}$ at large radii; both the luminosity and mass density in real galaxies fall off more slowly, as r^{-3} or r^{-2} . And recent observations of galactic nuclei demonstrate that constant-density cores do not exist – the density of starlight in real galaxies always rises monotonically at small radii, roughly as a power law.⁶ The density profile in these power-law “cusps” rises as steeply as $\rho \propto r^{-2}$ in faint elliptical galaxies, while the cusps in brighter galaxies are typically shallower.⁷ There is also increasingly strong evidence that many elliptical galaxies and bulges contain central massive objects, possibly the black holes that are thought to have powered quasars.⁸ While the masses of these dark central components are often very uncertain, typical estimates are $10^{-3} \lesssim M_{BH}/M_{gal} \lesssim 10^{-2}$, where M_{BH} is the black hole mass inferred from the orbital motions of surrounding stars and gas, and M_{gal} is the stellar mass of the host galaxy or (in the case of a spiral galaxy) the mass of the stellar bulge. Some galaxies, like M32, the dwarf companion to the nearby Andromeda galaxy, are known to contain both a steep stellar cusp ($\rho \propto r^{-1.6}$) and a dynamically-significant black hole ($M_{BH}/M_{gal} \sim 0.003$).

The existence of box orbits in the Perfect Ellipsoid is tied to the stability of the long-, or x -axis orbit.⁹ The x -axis orbit is unstable at most energies to lateral perturbations in triaxial models where the density increases more rapidly than $\sim r^{-1}$ near the center.¹⁰ The instability first appears through the bifurcation of a 1 : 2 resonant orbit, the $x - z$ “banana” boxlet.¹¹ The x -axis orbit is likewise unstable in any triaxial model with a central singularity.¹² It follows that bona-fide box orbits do not exist in the majority of triaxial potentials corresponding to real elliptical galaxies; in their place, we would expect to find either stochastic orbits, or regular orbits associated with minor resonances (like the banana) that avoid the center.

The non-existence of box orbits has important consequences for the self-consistent dynamics of elliptical galaxies. Schwarzschild^{13,14} and Statler¹⁵ found that box orbits – particularly the thin boxes that remain close to the long axis – were crucial for reconstructing the distribution of mass in triaxial models. Their work was based on mass models with smooth cores. Merritt & Fridman¹⁶ attempted to construct self-consistent triaxial models with central density cusps, after excluding the stochastic boxlike orbits, or replacing them with invariant ensembles representing a uniform population of stochastic phase space. Completely stationary solutions could not be found; only quasi-equilibrium solutions, in which stochastic phase space was populated in a non-uniform way, could successfully reproduce the density at all points in the model. An extension of this

work to triaxial models with a range of axis ratios¹⁷ revealed that stationary models with r^{-2} cusps could only be constructed if the figure was nearly axisymmetric.

One important question left unanswered by these equilibrium studies is the timescale over which chaos implies changes in the self-consistent structure of a galaxy. Here, results from two recent studies that address this question^{18,19} are presented.

2. Diffusion of Stochastic Orbits

In order for chaos to be relevant to real galaxies, it must produce a significant change in the region visited by an orbit after just a few tens or hundreds of orbital periods – the approximate lifetime of a galaxy. In a pioneering study, Goodman & Schwarzschild⁹ found that the boxlike orbits in a triaxial model with a smooth core were often stochastic, but that the orbital motion was essentially regular for at least 50 oscillations. On the other hand, Merritt & Fridman¹⁶ found that the stochasticity in triaxial models with $\rho \propto r^{-2}$ density cusps produced significant changes in the appearance of boxlike orbits after just a few tens of oscillations. Merritt & Valluri²⁰ went on to calculate timescales for mixing in these strongly chaotic potentials; they found that ensembles of stochastic trajectories evolved toward invariant distributions – corresponding to an approximately uniform filling of stochastic phase space – on timescales of only $10^1 - 10^2$ orbital periods. Taken together, these results suggest that the characteristic time over which chaos manifests itself in the orbital motion is strongly dependent on the central concentration of a triaxial model. Presumably, this dependence reflects the sensitivity of boxlike orbits to deflections that occur during close passages to the galaxy center.

A useful way to quantify the diffusion of stochastic orbits has been described by Laskar.^{21,22} His “frequency mapping” technique is based on the fact that a regular orbit can be characterized by the three fundamental frequencies ω_i , $i=1,2,3$ that define motion on an invariant torus. These frequencies can be computed with high accuracy by integrating an orbit for a finite length of time ΔT , storing its phase-space coordinates at regular intervals, and decomposing the motion into Fourier components. Carrying out this procedure for a large number of orbits at a given energy and plotting ω_1/ω_3 vs. ω_2/ω_3 gives the “frequency map,” a regular grid of points in frequency space. The same procedure can be carried out for stochastic orbits, but now the values of the ω_i will depend on the integration interval – a stochastic orbit is not confined to a single invariant torus and its “characteristic frequencies” will change with time as it diffuses along the energy surface. A strongly chaotic orbit will migrate through frequency space in just a few orbital periods, while a weakly chaotic orbit can remain close to a single invariant torus for a very long time. The diffusion is apparent as a distortion of the frequency map; the size of the distortion is proportional to the distance that the orbits have moved in frequency space during the period of integration ΔT .

Papaphilippou & Laskar^{23,24} demonstrated the usefulness of the frequency mapping technique for galaxy dynamics by using it to study orbital motion in the logarithmic potential,

$$\Phi(x, y, z) = \log(m^2 + r_c^2), \quad m^2 = \frac{x^2}{a^2} + \frac{y^2}{b^2} + \frac{z^2}{c^2}. \quad (1)$$

Equation (1) is the gravitational potential generated by a triaxial mass model in which the density falls off as r^{-2} outside of the core radius r_c . Papaphilippou & Laskar established that the motion of boxlike orbits in the logarithmic potential is generically chaotic, and showed that much of the chaos is associated with motion out of the principal planes.

A mass model that better represents the distribution of starlight near the centers of elliptical galaxies and bulges is Dehnen's law,²⁵

$$\rho(m) = \rho_0 m^{-\gamma} (1 + m)^{-(4-\gamma)}. \quad (2)$$

Dehnen's formula allows the steepness of the central density cusp to be adjusted through the parameter γ – a useful feature, since real elliptical galaxies and bulges have cusps with a range of slopes, $0 \lesssim \gamma \lesssim 2$. Figure 1 shows frequency maps of boxlike orbits in triaxial potentials derived from Dehnen's density law, with $c/a = 1/2$ and $b/a = 0.79$, and five different values of γ . All the orbits in a given map have the same energy, corresponding roughly to the gravitational potential at the half-mass radius. The fundamental frequencies were computed over a time interval ΔT equal to 50 periods of the x -axis orbit – roughly a galaxy lifetime. Approximately 10^4 orbits were integrated for each map; the initial conditions consisted of a grid of points distributed uniformly over the equipotential surface.¹⁸

The frequency maps of Figure 1 show a clear transition from nearly regular behavior over 50 orbital periods when $\gamma = 0$ or 0.5, to clearly chaotic motion when $\gamma = 1.5$ or 2. Many of the orbits can be seen to lie in resonance zones, regions associated with rational resonant layers $l\omega_1 + m\omega_2 + n\omega_3 = 0$, which appear as lines in the frequency maps. The last resonance to strongly influence the motion as γ approaches 2 is the 1 : 2 x - z banana resonance, which generates the vertical lines $\omega_1/\omega_3 = 0.5$ in Figure 1. For smaller values of γ the motion is influenced by a number of different resonances, some of rather high order.

By computing the fundamental frequencies over two adjacent time intervals, each of length ΔT , one can define a rate of diffusion in frequency space $\Delta\omega/\Delta T = \max\{|\Delta\omega_i|, i=1,2,3\}/\Delta T$.²⁶ The distribution of $\Delta\omega$'s is shown in Figure 3 for each set of orbits used in the construction of the frequency maps of Figure 1. Remarkably, there are no separate peaks associated with regular orbits, i.e. orbits with constant ω 's (such orbits would be expected to have $\Delta\omega/\omega_0 \approx 10^{-4}$, the approximate accuracy of the numerical routine that calculates the fundamental frequencies.) Instead, the spectrum of diffusion rates continues to rise toward small $\Delta\omega$, roughly as a power law. While there undoubtedly exist regular boxlike orbits associated with stable resonances like the

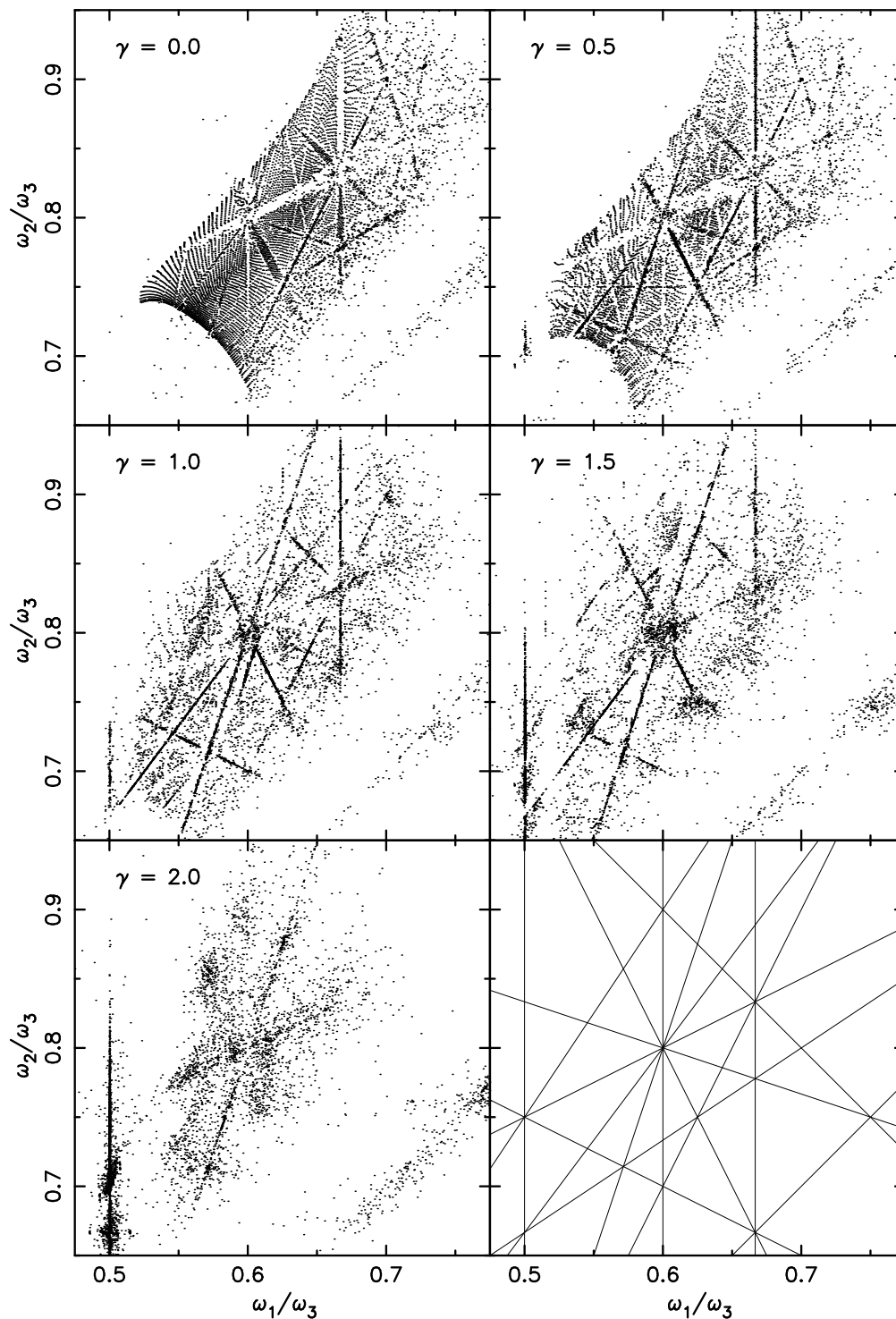


Figure 1. Frequency maps of boxlike orbits in triaxial potentials corresponding to the mass distribution of Eq. (2), with various cusp slopes γ .¹⁸ ω_1, ω_2 and ω_3 are the fundamental frequencies associated with oscillations along the long, intermediate and short axes of the triaxial ellipsoid. The nearly regular grid of points in the upper left-hand panel indicates that most of the orbits in the $\gamma = 0$ model mimic regular orbits over 50 oscillations. Departures from a regular grid imply that diffusion has taken place in frequency space, i.e. that the motion is stochastic. The bottom right panel shows the most important resonance layers, defined by $l\omega_1 + m\omega_2 + n\omega_3 = 0$ with integer $\{l, m, n\}$.

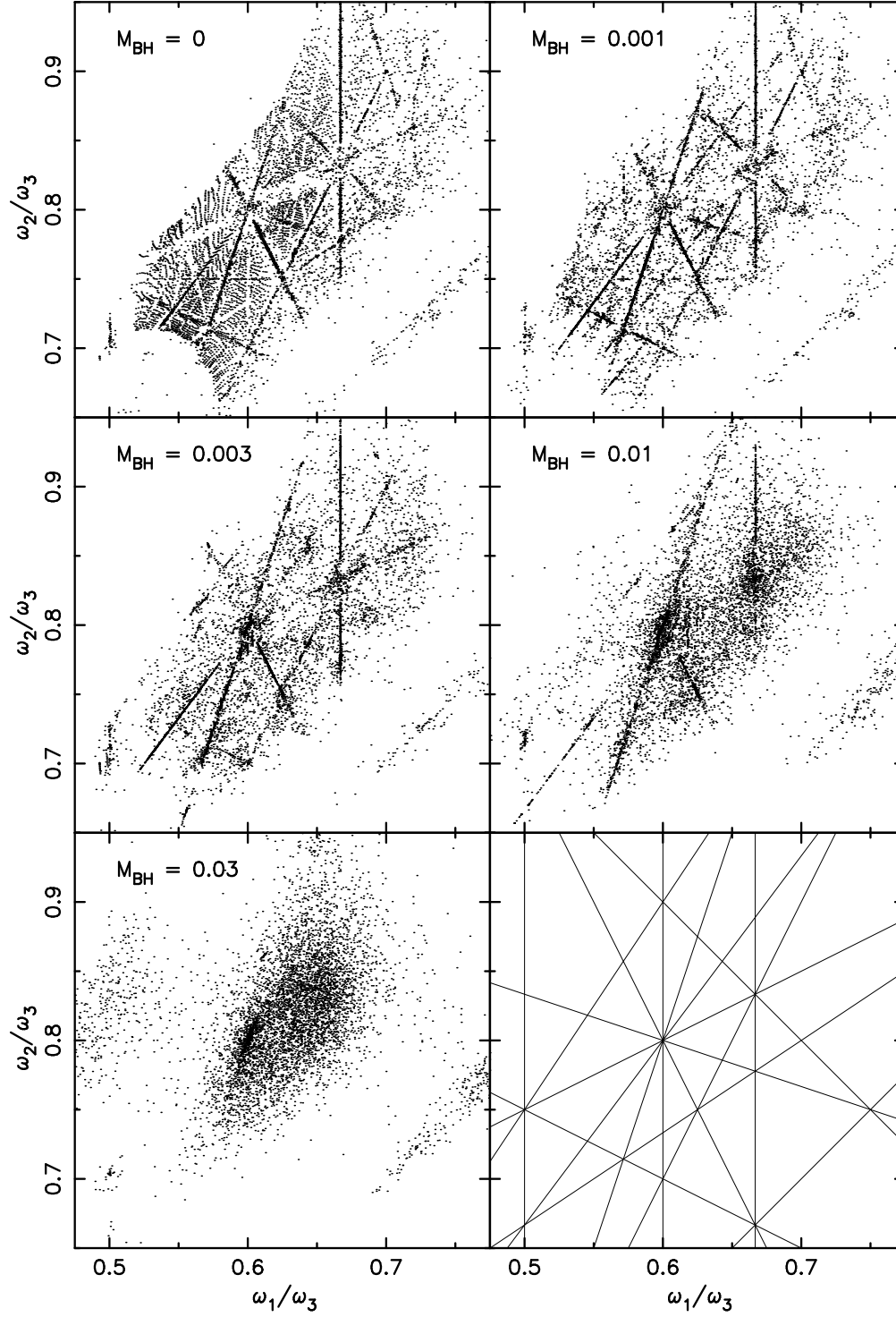


Figure 2. Like Figure 1, for boxlike orbits in Dehnen's model (Eq. 2) with $\gamma = 0.5$ and with an added central point mass containing various fractions M_{BH} of the total mass of the model.¹⁸

banana, Figure 3 suggests that the phase space volume associated with such orbits is very small. As γ approaches zero, the slope of the distribution increases, i.e. a smaller fraction of the boxlike orbits exhibit strong diffusion. But even for $\gamma = 0$ there is no hint of a separate population of regular orbits – rather, the typical diffusion times become much longer than 50 orbital periods, indicating that the majority of boxlike orbits are trapped for long periods of time in narrow regions of phase space.

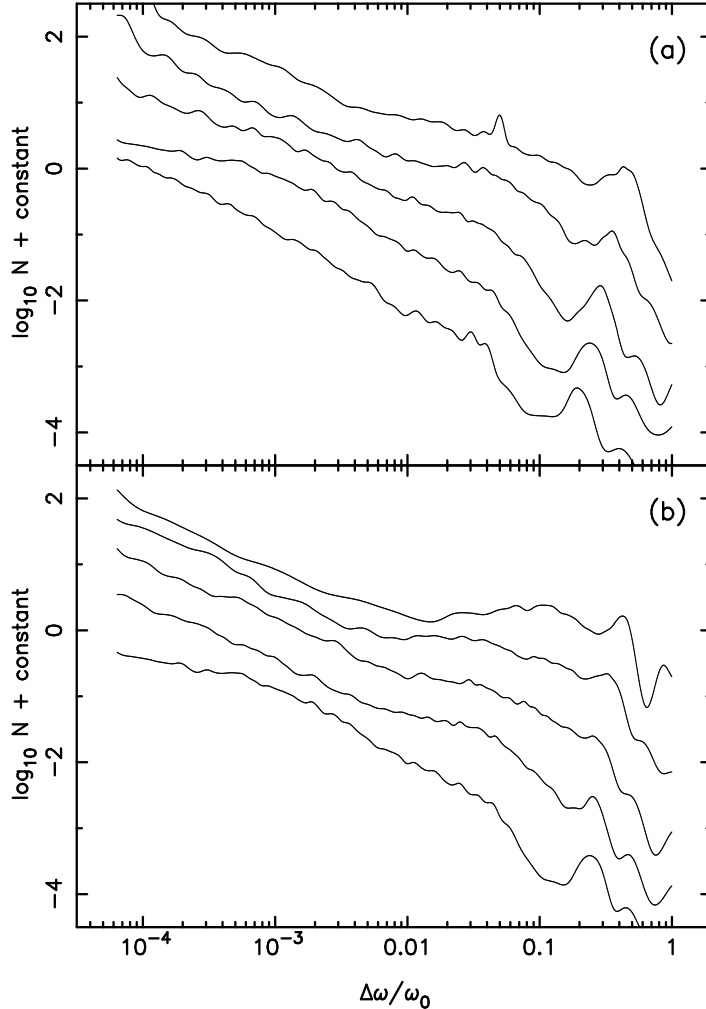


Figure 3. Spectra of diffusion rates for the orbits plotted in (a) Figure 1 and (b) Figure 2. The model parameters γ and M_{BH} increase upward. $\Delta\omega$ is the change in fundamental frequencies over 50 orbital periods; ω_0 is the frequency of the long-axis orbit.

These results suggest that the motion of boxlike orbits in triaxial potentials is generically chaotic, but that the distribution of diffusion rates varies systematically with the degree of central concentration of the model. In models with low central concentrations, typical diffusion times are long compared to 50 orbital periods, but as the central concentration is increased, a larger fraction of the

orbits are able to diffuse significantly in a galaxy lifetime. A very crude index of the importance of the diffusion can be defined as the fraction of boxlike orbits for which $\Delta\omega/\omega_0 > 0.1$, i.e. the fraction of orbits which experience a 10% or greater change in their fundamental frequencies over 50 orbital periods. Figure 4 shows that this fraction increases from $\sim 10\%$ at $\gamma = 0$ to $\sim 20\%$ at $\gamma = 1$ and $\sim 50\%$ at $\gamma = 2$. Thus, a typical boxlike orbit is essentially regular over the lifetime of a galaxy in triaxial potentials with $\gamma \lesssim 1$, and essentially chaotic when $\gamma \approx 2$. This conclusion is consistent with the very different configuration-space appearance of boxlike orbits integrated in triaxial potentials with cores⁹ and with steep cusps¹⁶.

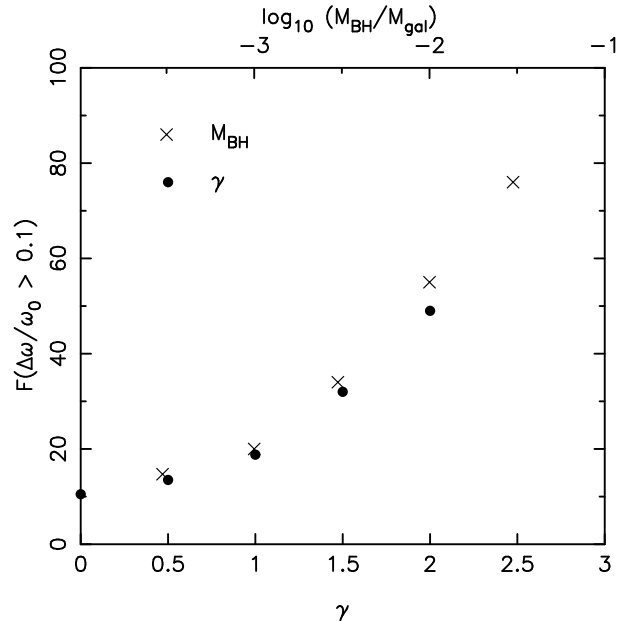


Figure 4. Fraction of boxlike orbits that undergo strong diffusion, $\Delta\omega/\omega_0 \geq 0.1$, in 50 orbital periods.

The effect of a central singularity on the frequency maps is shown in Figure 2, computed from Dehnen’s $\gamma = 0.5$ model with an added central point mass. When the black hole mass M_{BH} is less than about 0.1% of the galaxy mass, the frequency map differs only slightly from that of the model with $M_{BH} = 0$. As M_{BH} is increased to 1%, the motion becomes clearly chaotic, and for $M_{BH} = 3\%$ there is hardly a trace of structure remaining in the frequency map. Figure 3 verifies that the spectrum of diffusion rates becomes very shallow for large M_{BH} , even increasing toward large $\Delta\omega$ when $M_{BH} \gtrsim 0.3\%$. The fraction of boxlike orbits undergoing strong diffusion is illustrated in Figure 4; for $M_{BH} = 3\%$, fully 3/4 of the orbits evolve strongly over 50 orbital periods.

The frequency maps paint a more complex picture of the phase space of triaxial potentials than was apparent from earlier studies based on cruder techniques for characterizing the stochasticity. For instance, instability timescales of boxlike orbits inferred from Liapunov exponents are only 3 – 5 orbital periods

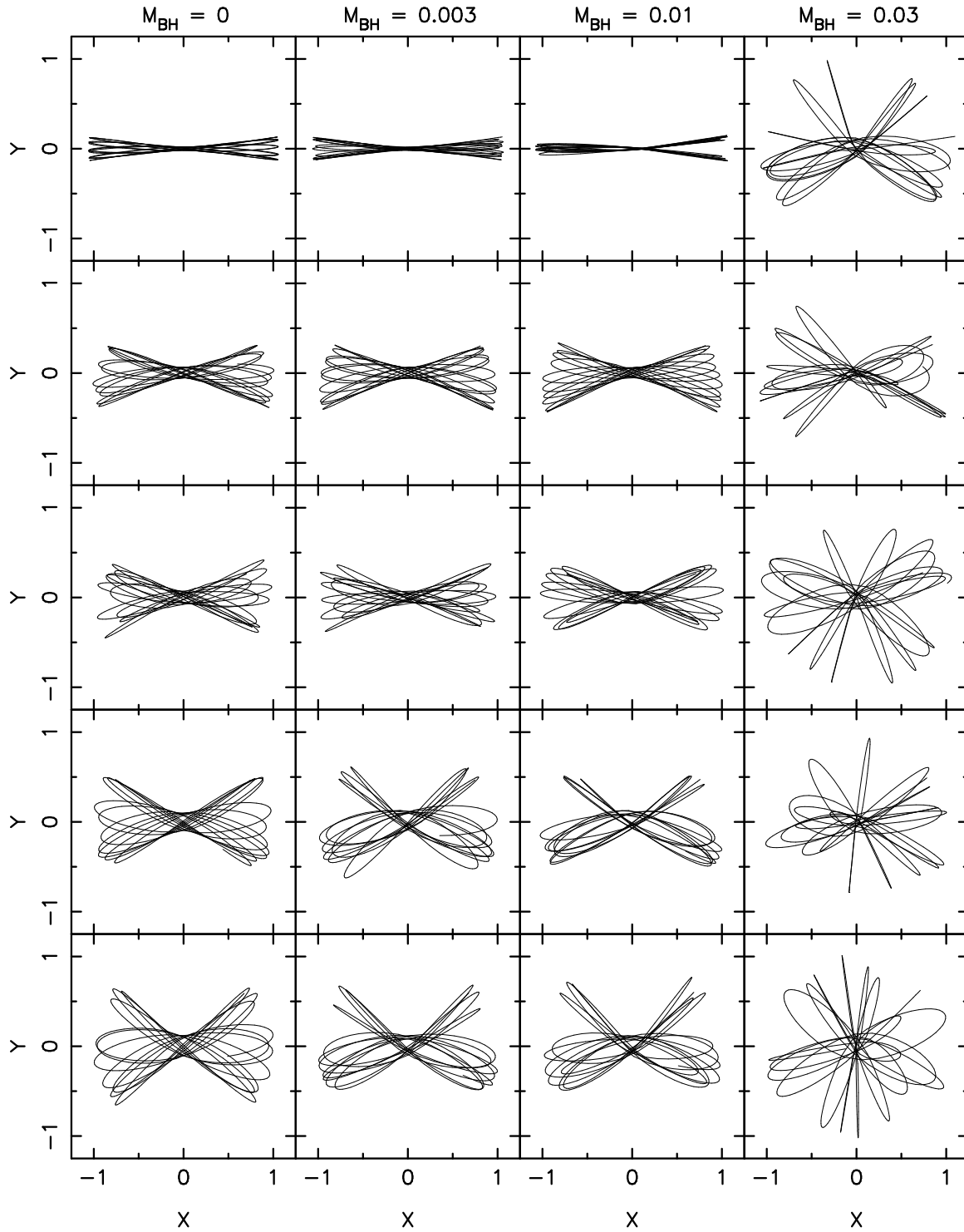


Figure 5. Test-particle integrations in a triaxial model with a smooth core and a central black hole. The z -axis is the short axis of the figure. Each of the five orbits is defined by its starting point on the equipotential surface, which remained fixed in angular position as M_{BH} was increased. Orbits were integrated for approximately 10 full oscillations. Chaos induces substantial changes in the orbital shapes over this period of time when $M_{\text{BH}} \gtrsim 0.02M_{\text{gal}}$.

in triaxial models like those studied here, even in models with smooth cores.²⁰ This is much shorter than the typical diffusion time inferred from the frequency map analysis. The apparent discrepancy can be understood by recognizing that the motion in weakly chaotic potentials is confined over long periods of time to narrow regions in phase space. The Liapunov exponents measure only the divergence rate of nearby trajectories within these limited regions, and not the physically more interesting timescale for diffusion from one such region to another. As the degree of central concentration of the model is increased, the stochastic layers increase in size until they overlap, and a large fraction of the boxlike orbits are able to wander ergodically over the energy surface in a finite length of time. This change in the structure of the phase space is reflected in the spectrum of diffusion rates, which becomes shallower as γ or M_{BH} are increased.

Dynamical systems often exhibit a transition to “global stochasticity”: as a perturbation parameter is increased, there is a sudden change from a regime in which the stochastic motion is closely bounded by KAM surfaces, to a regime where the stochastic motion is interconnected over large portions of the phase space. (Stochastic phase space in a 3 DOF system is always interconnected through the Arnold web, but Arnold diffusion is extremely slow unless the stochastic regions overlap.) In the globally-stochastic regime, there are few barriers to the motion, and stochastic orbits can wander over the full energy surface in little more than an orbital period. Is there a transition to global stochasticity in the triaxial models discussed here? Hints of such a transition can be seen in Figure 4, which shows that the fraction of boxlike orbits that evolve strongly in 50 orbital periods becomes large as M_{BH} is increased beyond about $0.01M_{gal}$. In fact the situation is even more dramatic than this, as illustrated in Figure 5, which shows the behavior of boxlike orbits integrated for just 10 orbital periods in triaxial models with a smooth core and various values of M_{BH}/M_{gal} . When the black hole mass exceeds $\sim 2\%$ of the galaxy mass, orbital evolution takes place in only a few oscillations – just the behavior expected in the globally-stochastic regime. If one imagines slowly increasing the mass of a black hole at the center of a triaxial galaxy, Figure 5 suggests that the galaxy would be forced to respond very rapidly – perhaps in just a few crossing times – once the black hole mass exceeded $\sim 0.02 M_{gal}$.

3. Self-Consistent Evolution

In recent studies of the triaxial self-consistency problem^{16,17,27}, attempts were made to identify the stochastic orbits and to treat them differently from the regular orbits in the model construction. The separation of regular from stochastic orbits in these studies was based on the detection of linear instability of the motion; regular orbits were defined simply as those that showed no clear evidence of instability over ~ 100 oscillations. But the true situation is more complex, as discussed above. Boxlike orbits exhibit a wide range of diffusion rates, with no clear separation into “regular” and “stochastic” families. In addition, orbital periods decrease toward the center of a galaxy; an orbit with a diffusion timescale of 10^3 periods would mimic a regular orbit in the outer parts of a galaxy, but

would behave chaotically over a galaxy lifetime if located near the center.

There would seem to be no substitute for N -body codes when dealing with a situation as complex as this. Until recently, N -body algorithms were unable to deal in a practical way with the high degree of central concentration of realistic triaxial models. But the situation has changed, and a number of algorithms are now available that can efficiently represent the gravitational potentials of systems with central cusps and nuclear black holes.²⁸ Here, the results of a new N -body study¹⁹ of triaxial galaxies with central singularities is presented.

The initial conditions for this study consisted of $\sim 10^5$ particles distributed in a nonrotating triaxial bar, with $c/a \approx 0.5$ and $b/a \approx 0.75$. The initial model was generated by collapsing a cold, spherical cloud and allowing it to evolve to an equilibrium state; the triaxial shape resulted from a bar-making instability associated with cold collapse.²⁹ In order to increase the resolution very near the center, particles were given masses that depended on their initial positions; masses varied by a factor of 10 from the center to the envelope. Particle positions were advanced with individual timesteps, sometimes differing by as much as a factor of 10^6 , using a fourth-order integrator.

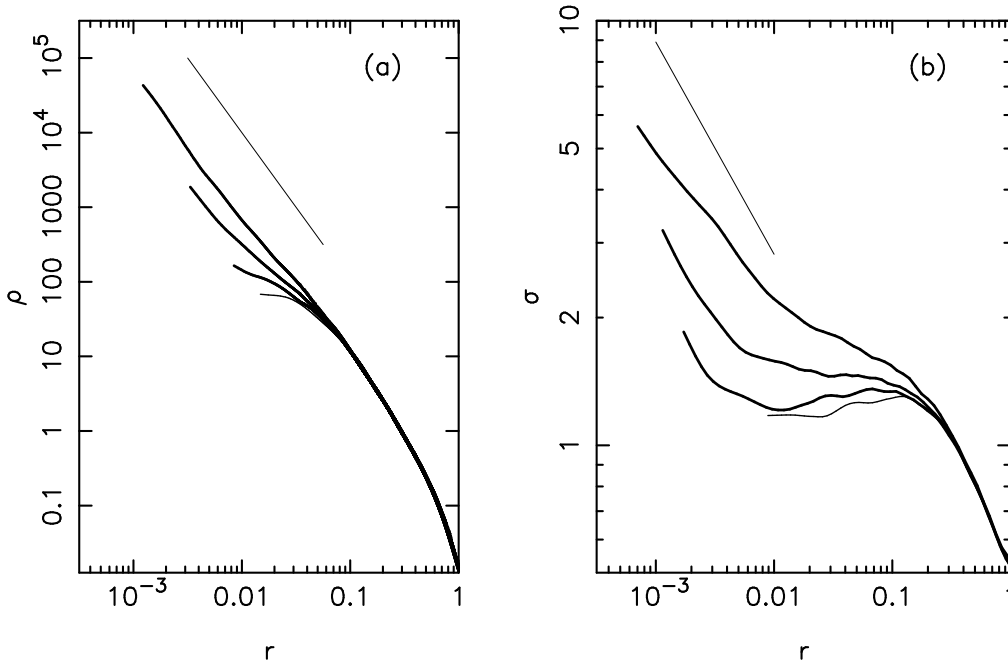


Figure 6. Growth of central density cusps in N -body models with various black hole masses.¹⁹ (a) Density profiles; (b) velocity dispersion profiles. The thin curve is the initial model without a black hole; the three heavy curves are final models with $M_{BH}/M_{gal} = 0.003, 0.01, 0.03$. The straight line in panel (a) has a logarithmic slope of -2 ; in panel (b), of -0.5 .

The initial model had a constant-density core. A “black hole” was grown in this core by increasing the mass at the origin according to $M(t) = M_{BH}\tau^2(3 - 2\tau)$, with $\tau = t/t_{grow}$. Various values for M_{BH} and t_{grow} were used. Figure 6 illustrates the formation of a density cusp in the stars surrounding the black

hole; the cusp forms because the black hole pulls in the neighboring stars as the force of its attraction increases.³⁰

The growth of a black hole in an initially triaxial model is expected to make the model more axisymmetric, through a two-step process.^{31,32} Many of the box orbits in the initial model are rendered stochastic by the black hole; as a result, they evolve to fill a more-or-less spherical volume corresponding roughly to the region enclosed by an equipotential surface. Nearly-spherical orbits are not very useful for reconstructing a barlike shape, and so the model responds by becoming more axisymmetric. As it approaches axisymmetry, the tube orbits that circulate about the symmetry axis are able to reproduce the mass distribution self-consistently and the galaxy settles rapidly into equilibrium.

This picture appears to be essentially correct, as illustrated in Figure 7, which shows the evolution of the intermediate-to-short axis ratio b/a of the model as the black hole is grown. For three different black hole masses, $M_{BH}/M_{gal} = 0.3\%, 1\%$ and 3% , the model evolves to a final state that is almost precisely axisymmetric. The short-to-long axis ratio also increases, from its initial value of ~ 0.5 , to ~ 0.9 near the center and ~ 0.6 at the half-mass radius; the elongation of the model ceases to change once axisymmetry is reached, a fact which argues in favor of the evolution being driven by the box orbits.

Although the final shape of the model is nearly the same for the three different values of M_{BH} tested here, the evolution time was found to depend strongly on the black hole mass. When $M_{BH} = 0.003M_{gal}$, axisymmetry was not quite reached by the end of the integration, at roughly 55 half-mass orbital periods. But when M_{BH} was increased to $0.03M_{gal}$, the model evolved in shape on approximately the same timescale that the black hole grew. Experiments with smaller values of t_{grow} revealed that the response time of the galaxy to the black hole was essentially instantaneous – i.e., of order the local orbital period – when M_{BH} exceeded $\sim 2\%$ of the galaxy mass. Such rapid evolution is just what would be expected based on the test particle integrations shown in Figure 5. We conjecture that a transition to global stochasticity occurs at $M_{BH} \approx 0.02 M_{gal}$, causing the boxlike orbits to lose their characteristic shapes in a single orbital period. The galaxy responds by rapidly becoming axisymmetric.

This rapid evolution toward axisymmetry may constitute a negative feedback mechanism that determines the maximum mass of nuclear black holes.¹⁹ In one widely-discussed scheme,³³ nuclear black holes grow by capturing stars or gas clouds on box orbits as they pass near the galactic center. But as the mass of the black hole approaches $\sim 2\%$ of the galaxy’s mass, the galaxy would evolve rapidly to axisymmetry, thus eliminating the box orbits and cutting off the supply of stars or gas to the black hole. Black holes could then never accrete more than $\sim 2\%$ of their host galaxy’s mass unless they somehow managed to grow on a timescale much shorter than a galaxy crossing time. This hypothesis is consistent with what is known so far about the masses of nuclear black holes, the largest of which have masses of order 1% the stellar mass of their parent galaxies.⁸ The current record-holder is NGC 3115,³⁴ which has $M_{BH}/M_{gal} \approx 2.5\%$, nicely consistent with the prediction.

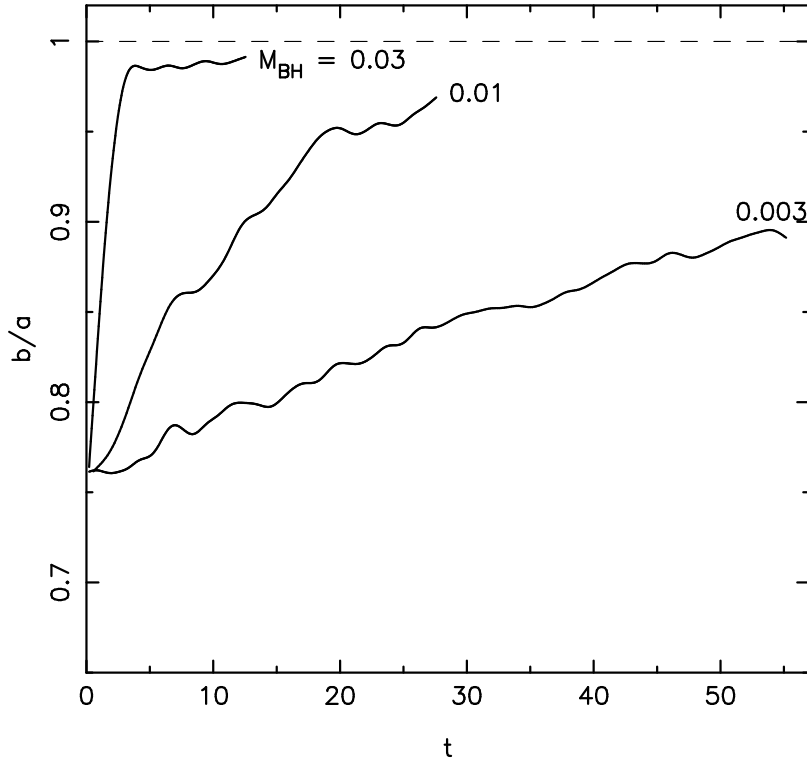


Figure 7. Evolution of the intermediate-to-long axis ratio b/a of the N -body models as nuclear black holes of three different masses are grown.¹⁹ Time is in units of the half-mass orbital period. Black hole masses are expressed in terms of the total mass of the galaxy model. The axis ratio was computed from the most-bound 50% of the stars. The two smaller black holes were grown on a timescale of 5 half-mass orbital periods; the black hole with $M_{BH} = 0.03$ was grown in 2 half-mass orbital periods.

Although the critical black hole mass found here was derived from a single triaxial model with a particular shape, roughly the same mass may define the transition to global stochasticity in models with very different geometries. For instance, Norman, Sellwood & Hasan³⁵ found that 2-D models of rotating barred spiral galaxies exhibited strong evolution toward axisymmetry when M_{BH}/M_{gal} exceeded $\sim 5\%$. But in 3-D simulations of similar barred systems,³⁶ the bar was found to be much more fragile, evolving strongly once the black hole mass fraction exceeded $\sim 1\%$.

The N -body work described here was carried out in collaboration with G. Quinlan. We thank J. Sellwood for helpful comments on the manuscript. This work was supported by NASA grant NAG 5-2803 and by NSF grants AST 93-18617 and AST 96-17088.

References

1. Chandrasekhar, S. 1942. Principles of Stellar Dynamics. University of Chicago Press. Chicago, IL.
2. Hunter, C. 1995. Ann. NY Acad. Sci. **751**: 76
3. Kuzmin, G. G. 1956. Astr. Zh. **33**: 27
4. Kuzmin, G. G. 1973. Quadratic Integrals of Motion and Stellar Orbits in the Absence of Axial Symmetry of the Potential. *In* Dynamics of Galaxies and Clusters. T. B. Omarov, Ed.: 71. Akad. Nauk. Kaz. SSR. Alma Ata.
5. de Zeeuw, P. T. 1985. Mon. Not. R. Astron. Soc. **216**: 273.
6. Gebhardt et al. 1996. Astron. J. **112**: 105.
7. Merritt, D. & T. Fridman. 1995. Equilibrium and Stability of Elliptical Galaxies. *In* Fresh Views of Elliptical Galaxies, A. S. P. Conf. Ser. Vol. **86**. A. Buzzoni, A. Renzine & A. Serrano, Eds.: 13-22. Astronomical Society of the Pacific. Provo, Utah.
8. Kormendy, J. & D. O. Richstone. 1995. Ann. Rev. Astron. Astrophys. **33**: 581.
9. Goodman, J. & M. Schwarzschild. 1981. Astrophys. J. **245**: 1087.
10. Fridman, T. & D. Merritt. 1997. Astron. J. **114**: in press.
11. Miralda-Escudé, J. & M. Schwarzschild. 1989. Astrophys. J. **339**: 752.
12. Gerhard, O. & J. J. Binney. 1985. Mon. Not. R. Astron. Soc. **216**: 467.
13. Schwarzschild, M. 1979. Astrophys. J. **232**: 236.
14. Schwarzschild, M. 1982. Astrophys. J. **263**: 599.
15. Statler, T. 1987. Astrophys. J. **321**: 113.
16. Merritt, D. & T. Fridman. 1996. Astrophys. J. **460**: 136.
17. Merritt, D. 1997. Astrophys. J. **486**: in press.
18. Valluri, M. & D. Merritt. 1997. Rutgers Astrophysics Preprint Series No. 214.
19. Merritt, D. & G. Quinlan. 1997. Rutgers Astrophysics Preprint Series No. 212.
20. Merritt, D. & M. Valluri. 1996. Astrophys. J. **471**: 82.
21. Laskar, J., C. Froeschlé & A. Celletti. 1992. Physica D **56**: 253.
22. Laskar, J. 1996. Introduction to Frequency Map Analysis. *In* NATO-Advanced Study Institute, Hamiltonian Systems with Three or More Degrees of Freedom. C. Simo & A. Delshams, Eds.
23. Papaphilippou, Y. & J. Laskar. 1996. Astron. Astrophys. **307**: 427.
24. Papaphilippou, Y. & J. Laskar. 1997. Astron. Astrophys. in press.
25. Dehnen, W. 1993. Mon. Not. Royal Astron. Soc. **265**: 250.
26. Laskar, J. 1993. Physica D **67**: 257.
27. Schwarzschild, M. 1993. Astrophys. J. **409**: 563

28. Sellwood, J. A. 1997. Galaxy Dynamics by N -Body Simulation. *In* Computational Astrophysics, A. S. P. Conf. Ser. Vol. **123**. D. A. Clarke & M. J. West, Eds.: 215-220. Astronomical Society of the Pacific. Provo, Utah.
29. Aguilar, L. & D. Merritt. 1990. *Astrophys. J.* **354**: 33.
30. Peebles, P. J. E. 1972. *Gen. Rel. Grav.* **3**: 63.
31. Gerhard, O. & J. Binney. 1995. *Mon. Not. Royal Astron. Soc.* **216**: 467.
32. Norman, C. A., A. May & T. S. van Albada. 1985. *Astrophys. J.* **296**: 20.
33. Norman, C. A. & J. Silk. 1993. *Astrophys. J.* **266**: 502.
34. Kormendy, J., R. Bender & S. Tremaine. 1996. *Astrophys. J.* **459**: L57.
35. Norman, C. A., J. A. Sellwood & H. Hasan. 1996. *Astrophys. J.* **462**: 114.
36. Sellwood, J. A. & E. Moore, in preparation.